JOURNAL OF OPTOELECTRONICS AND ADVANCED MATERIALS Vol. 10, No. 11, November 2008, p. 3069 - 3076

Problems and solutions in electrolyte crystal growth kinetics

HANS E. LUNDAGER MADSEN
Department of Basic Science and Environment, Faculty of Life Sciences, University of Copenhagen, Thorvaldsensvej 40, DK-1871 Frederiksberg C, Denmark

As far as crystal growth is concerned, electrolytes differ from nonelectrolytes in several aspects, of which the most important are that a growth unit consists of more than one particle, and that interactions between ions are of long range. This raises questions about the validity of current theories and calls for modifications of kinetic expressions. On the other hand, electrolyte systems offer possibilities of convenient experimental methods such as recording of electrical conductance or electrode potentials during a crystallization process. Practical examples from studies of sparingly soluble carbonates and phosphates are presented and discussed.

(Received August 5, 2008; accepted October 30, 2008)

Keywords: Electrostatic interactions, Edge free energy, Spiral growth, Surface nucleation, Conductometry, pH recording

1. Introduction

When theories of crystal growth kinetics were first established, they were based on nonelectrolytes. There are two obvious reasons for that: first, that in this case growth units are single molecules, and second, that interactions between neutral molecules fall off with distance so quickly that it is a reasonable approximation to consider only interactions between nearest neighbours in the crystal. A growth unit of an electrolyte consists of at least one cation and one anion like e.g. AgCl or $BaSO_4$, and often more, for instance a total of 9 for apatite, $Ca_5OH(PO_4)_3$. The electrostatic interaction between ions is of much longer range than the interaction between neutral molecules, which is furthermore always attractive except at very close approach, whereas ions of the same sign, as well known, repel each other. This makes the nearest-neighbour approximation very poor for electrolyte crystals.

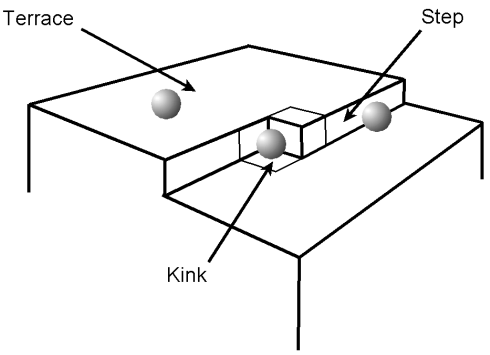

Fig. 1. Growing crystal.

We may illustrate the situation by considering a growing crystal with simple cubic structure (Fig. 1). When a growth unit or single ion is adsorbed at a regular lattice position on the terrace, it has 1 nearest neighbour, at the step it has 2 and at the kink (growth site) 3. If the nearest-neighbour interaction energy is φ (< 0), then the potential energies at the three sites are φ, 2φ and 3φ, respectively, in the nearest-neighbour approximation. For a single ion on a (100) face of an ionic crystal with NaCl structure Kossel [1] and Stranski [2] found the corresponding values 0.0662φ, 0.1807φ and 0.8738φ. For a whole growth unit, i.e. a pair of ions at neighbouring sites, the values are 1.1324φ, 1.3614φ and 1.7476φ. These values include purely electrostatic interactions only; a precise treatment should consider Born repulsion and dispersive and vibrational energies as well [3,4]. Finally, since electrolyte crystals often grow from aqueous solution, crystal-water interaction is important too [5,6].

With electrolytes of low solubility additional problems arise. First, such crystals often require much higher supersaturation to grow at a measurable rate than crystals of a highly soluble substance like NaCl or KH_2PO_4. This fact invalidates certain approximations frequently made to simplify kinetic analyses. For instance, the approximation $\ln \beta \approx \beta - 1$, where β is the saturation ratio (to be defined precisely below) is in error by more than 50 % for $\beta > 2.15$, which is a rather low supersaturation for a sparingly soluble electrolyte. Second, solutions from which crystal growth takes place need not be congruent, i.e. contain the ion constituents in the same proportion as in the crystal. Crystal growth kinetics of a biologically important compound like apatite, of which the growth unit consists of 5 Ca^{2+}, 3 PO_4^{3-} and 1 OH^-, is of interest chiefly in neutral medium (pH ≈ 7), where the dominating phosphate species are $H_2PO_3^-$ and HPO_4^{2-}, and the concentration of hydroxide ion is very low. Furthermore, in actual biological fluids the total phosphate concentration is often higher than that of calcium. This

forces us to focus on the question of rate-determining step with particular emphasis on the ionic species which limits growth rate.

On the other hand, electrolytes offer experimental methods not available for nonelectrolytes. Measurements of electrochemical properties like electrical conductance and electrode potential are particularly useful in mass crystallization experiments. In addition to a short account of such methods, the aim of the present contribution is to point out where and how current theories of crystal growth should be revised to account adequately for the growth of electrolyte crystals. Not everything that follows is novel, but the implications of specific electrolyte properties are often ignored even in recent work.

2. Basic theory of crystal growth from solution

The rate of growth R of a crystal is the velocity of advancement of a crystal face in the direction perpendicular to the face. If the crystal habit includes more than one form (set of symmetrically equivalent faces), different faces will normally have different growth rates. In a mass crystallization experiment the result will typically be an average growth rate.

2.1 Thermodynamics of dissolved electrolytes

The driving force for crystal growth from solution is the excess of chemical potential of the crystallizing solute over that of the crystal:

$$\Delta\mu = \mu - \mu^{\mathrm{c}} \tag{1}$$

where the chemical potential of an electrolyte equals the sum of the potentials of its ion constituents. Let the chemical formula be $\mathrm{M}_m\mathrm{X}_x$, then

$$\mu = m\mu_{\mathrm{M}} + x\mu_{\mathrm{X}} = m\mu_{\mathrm{M}}^{\ominus} + x\mu_{\mathrm{X}}^{\ominus} + RT\ln a_{\mathrm{M}}^{m}a_{\mathrm{X}}^{x} \tag{2}$$

where $\mu_{\mathrm{M}}^{\ominus}$ and $\mu_{\mathrm{X}}^{\ominus}$ are the standard chemical potentials and a_{M} and a_{X} the activities of the ion constituents in solution. In a saturated solution the chemical potential equals μ^{c}, and the ion activity product is the solubility product K_{sp}. If we define the saturation ratio β by

$$RT\ln\beta = \Delta\mu \tag{3}$$

we have

$$\beta = \frac{a_{\mathrm{M}}^{m}a_{\mathrm{X}}^{x}}{K_{\mathrm{sp}}} \tag{4}$$

Often supersaturation is expressed as mean saturation ratio per ion constituent, S. It is related to β by

$$\beta = S^{m+x} \tag{5}$$

For nonelectrolyte systems β and S are identical, and for a congruent solution S may be taken as the actual concentration of the electrolyte divided by its solubility, provided that the activity coefficients in the actual solutions are nearly equal to those of the saturated solution. This is often a reasonable assumption for highly soluble substances. Another way to determine S in such cases is to use the approximate relation [7]

$$\ln S = \frac{\Delta_{\mathrm{sol}}H}{RT_{\mathrm{eq}}^{2}}\Delta T \tag{6}$$

where the numerator is the integral heat (enthalpy) of solution of 1 mol of solute in the amount of solvent to give the actual concentration, and ΔT is the supercooling in K below the saturation temperature T_{eq}.

2.2 Kinetic growth laws

It is sometimes found that the growth rate R of a crystal is proportional to the relative supersaturation $\sigma = S - 1$ in a range of supersaturations. This is termed the linear growth law and is normally interpreted as the consequence of a high degree of roughness of the crystal surface, making volume diffusion the rate-determining step. Two other basic laws are generally recognized: the "parabolic" and the "exponential" law. The former draws its name from the fact that R is often proportional to σ^2 at low supersaturation. It is connected with the presence on the crystal face of a spiral-shaped step, a growth spiral, arising from a screw dislocation in the crystal. The theory of this growth mechanism was established by Burton, Cabrera and Frank [8] (BCF) and further developed by Chernov [9], Gilmer, Ghez and Cabrera [10], Bennema and Gilmer [11] and van der Eerden [12], among others. These versions of the theory of spiral growth all predict both first order (linear) and second order (parabolic) dependence of growth rate on relative supersaturation. Some of the special, limiting cases yield, however, an expression of the form

$$R = b(\beta - 1)\ln\beta \tag{7}$$

which for sufficiently low supersaturations may be approximated to $R = b\sigma^2$. b is a temperature-dependent rate constant.

The "exponential" law is a consequence of the mechanism of crystal growth by surface nucleation on a perfect crystal face or between the steps of a growth spiral. Nucleation means the formation of nuclei, which are groups or "islands" of growth units in contact with each other, but separated from other such groups. A small nucleus is unstable and will tend to dissolve, a large nucleus will tend to grow, and between the two is the critical nucleus, which is in unstable equilibrium with the surrounding medium. Its size is related to supersaturation

through the two-dimensional Gibbs-Kelvin equation

$$kT \ln \beta = \frac{\lambda \bar{s}}{r^*} \tag{8}$$

where λ is the edge free energy of the nucleus, i.e. the Helmholtz free energy per unit length of a monomolecular step, $\bar{s}$ is the area occupied by one growth unit at the crystal surface and r^* is the radius of a circular nucleus or half the edge length of a square nucleus. This quantity further determines the distance y_0 between steps of a growth spiral; we have

$$y_0 = 19 r^* \tag{9}$$

for both rounded and polygonized spirals [13,14]. The theory of surface nucleation dates back to the classical works of Becker and Döring [15] and of Volmer [16]. It was further developed for crystal growth from the vapour by Kaischev [17], whose expression for the frequency per unit area of two-dimensional nucleation per unit area on a crystal surface may be written

$$J = k_1 \beta (\ln \beta)^{1/2} \exp\left(- \frac{g \lambda^2 \bar{s}}{(kT)^2 \ln \beta} \right) \tag{10}$$

where g is a geometric factor equal to 4 for a square nucleus and π for a circular nucleus.

If only one growing embryo were present on the crystal face at a time, then growth rate R would be proportional to the rate of two-dimensional nucleation as given by (10); this case is known as the mononuclear mechanism. However, R would also be proportional to the area of the face, meaning that crystal growth would accelerate with increasing crystal size. Such behaviour is not normally observed. To solve this problem Hillig [18] proposed for crystal growth from the melt the polynuclear mechanism, where several growing nuclei are present on the crystal face at the same time. R is then determined by both rate of nucleation J and rate of advancement v of growth steps across the crystal face, and we have

$$R = \left(\frac{4}{3} \right)^{1/3} J^{1/3} v^{2/3} d \tag{11}$$

where d is the thickness of a growth layer. From this relation Simon, Grassi and Boistelle [19] established for crystal growth from solution an expression which may be written

$$R = k_2 \beta^{1/3} (\beta - 1)^{2/3} (\ln \beta)^{1/6} \exp\left(- \frac{g \lambda^2 \bar{s}}{3(kT)^2 \ln \beta} \right) \tag{12}$$

Nielsen obtained a similar expression, but with β replaced by S and the first factor to the power of 7/6 instead of 1/3 [20].

As already indicated above, surface nucleation may take place on a perfect crystal face as well as between the steps of a growth spiral. The resulting growth rate is not simply the sum of the contributions from spiral growth and from surface nucleation. Instead, they combine according to Gilmer's equation [21]

$$\frac{R_n^3 \tau^3}{d^3} + \frac{R_s \tau}{d} = 1 \tag{13}$$

where R_n is the growth rate by surface nucleation only, and R_s is similarly the rate of spiral growth only. τ is the time it takes to fill completely a layer of thickness d; thus, the overall growth rate equals $R = d/\tau$.

2.3 Traditional approaches

It is not uncommon to see the term "parabolic" for the kinetic law of spiral growth taken literally. R is plotted as a function of S - 1 in a log-log plot and kinetics determined from the slope of the plot: 1 means linear law (rough surface), 2 means parabolic law (spiral growth), and a higher value means exponential law. This must be regarded as an oversimplification of crystal growth kinetics, which often leads to false conclusions. As a practical example we may consider the crystal growth kinetics of the cadmium phosphate $Cd_5H_2(PO_4)_4{,}4H_2O$ (Fig. 2), determined by mass crystallization experiments [22,23]. The growth unit consists of 9 ions: 5 Cd^{2+}, 2 HPO_4^{2-} and 2 PO_4^{3-}, so $\beta = S^9$. The slope of the dotted line marked "linear" is 1 and that of the dashed line marked "parabolic" is 2.

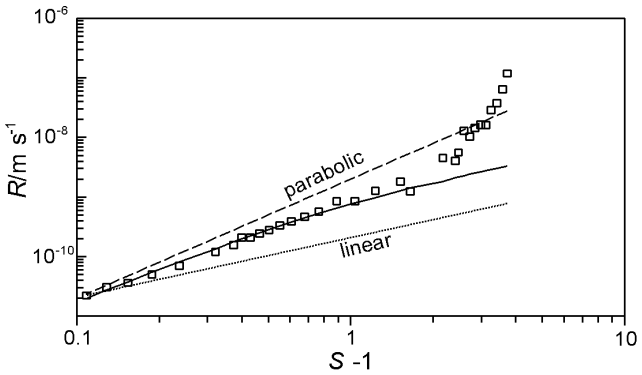

Fig. 2. Log-log plot of growth kinetics of cadmium phosphate crystals. Squares: experimental points. Full line: best fit f or spiral growth according to theory (see text).

It is evident from the graph that there is a change in kinetics above $S \approx 3$. It is also evident that neither the linear nor the parabolic growth law fits the experimental data. The expression for the curve of best fit will be given in the next section.

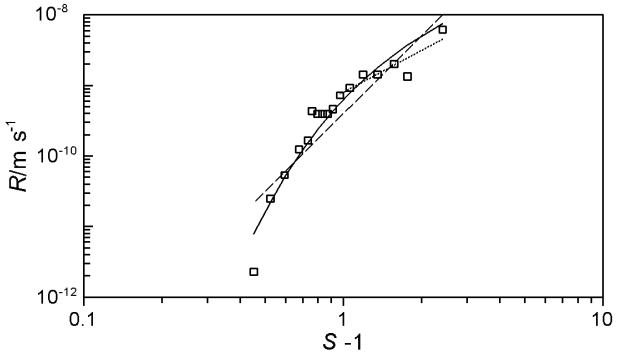

Fig. 3. Similar to Fig. 2, results from another experiment. Full line: best fit for surface nucleation kinetics (see text). Dashed and dotted lines: linear fits.

An example of the "exponential" law is shown in Fig. 3. The nonlinear dependence is evident. However, if a linear fit is made for the 7 points at highest supersaturation (dotted line), a slope not significantly different from 2 is found. This clearly illustrates the risk of false conclusions using this method.

A more rational approach in mass crystallization involves the notion of chronomals (chronometric integrals) originally introduced by O'Rourke and Johnson [24] and further developed by Nielsen [25,26]. However, its practical use is often based on simplyfying assumptions like those of the log-log plot, and generalizations are not straightforward [27].

3. Electrolyte crystal growth

We shall now consider in detail the problems and possibilities outlined in the Introduction, starting with a short account of the available experimental methods and then continue with modifications of the theory to deal with crystal growth of electrolytes. Assuming that we can take over the form of the rate expressions listed above, the primary question will be where to replace β by another quantity, e.g. S or a concentration or activity of a dissolved species. To solve this problem, it will be useful to group the occurrences in two categories: those of thermodynamic and those of kinetic origin.

3.1 Experimental methods

When highly soluble electrolytes are concerned, the methods used for studying crystal growth are essentially the same as those used for nonelectrolytes. One of the most frequently used methods consists in placing a seed crystal in a solution made supersaturated by cooling a saturated solution. Growth of the crystal is followed by direct observation through a microscope, often combined with measurement of birefringence [28] or use of contrast methods permitting observation of growth spirals on the growing crystal [29,30]. Additional information may be obtained from *in situ* x-ray topography [31] or interferometry [32,33]. In recent years *in situ* atomic force microscopy (AFM) has gained importance [34,35].

For sparingly soluble electrolytes sufficient supersaturation is not readily attained by changing the temperature of a saturated solution. Instead, two solutions are mixed, one containing the cation, the other the anion of the crystallizing substance, such as $AgNO_3$ and NaCl to produce AgCl, and $BaCl_2$ and Na_2SO_4 for $BaSO_4$. Furthermore, it is usually rather difficult to obtain a single crystal of such a size that it can be handled and mounted in a crystal growth cell. Most studies of crystal growth kinetics of sparingly soluble electrolytes are carried out as mass crystallization experiments, where a very large number of growing crystals is involved. Since ions leave the solution to enter the crystals, the electrical conductance decreases in the course of the process, which may accordingly be followed by conductometry. Fig. 4 shows how conductance κ varies when solutions of $Ca(OH)_2$ and HF are mixed to form fluorite, CaF_2 [36].

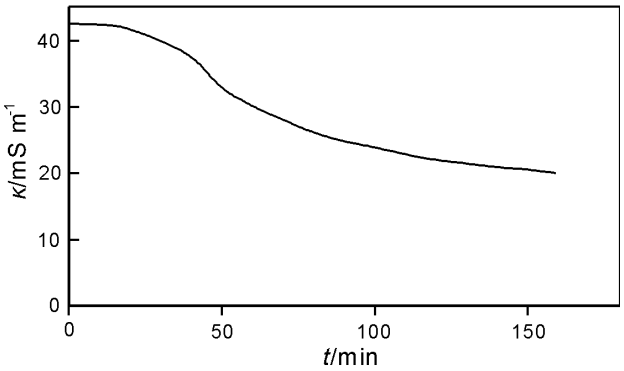

Fig. 4. Recorded conductance values in mass crystallization experiment with fluorite.

Another possibility exists for salts of weak acids crystallizing from neutral or acid solution, where the anion is protonized. For instance, the cadmium phosphate mentioned above crystallizes according to the reaction scheme

$$5\ Cd^{2+} + 4\ H_2PO_4^- + 4\ H_2O \rightarrow Cd_5H_2(PO_4)_4{,}4H_2O + 4\ H^+$$

and the protons liberated in the process will lower pH of the solution. Knowing the solubility product of the crystallizing phase and the dissociation constants of phosphoric acid as well as other relevant equilibrium constants of the system, it is possible from the recorded pH values to calculate the residual supersaturation and the amount of solid crystallized at any time during the process. Fig. 5 shows recorded pH values versus time for the experiment, of which the kinetic results are illustrated in Fig. 2 [23].

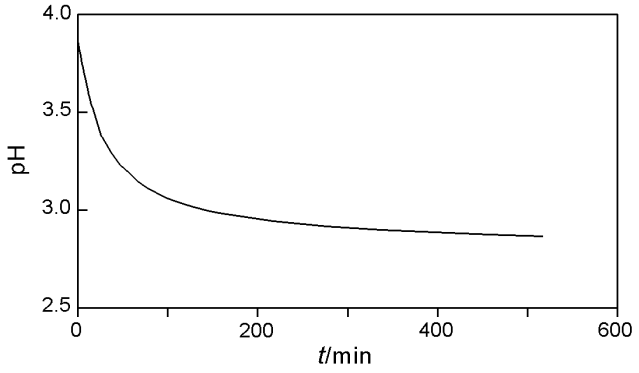

Fig. 5. pH recording in cadmium phosphate crystallization experiment.

Crystal growth may be initiated either by free crystallization, in which solutions are mixed and the growth of the crystals actually formed is studied, represented by the above studies of fluorite and cadmium phosphate, or by seeding, i.e. adding to a supersaturated solution a sample of well-characterized crystals. The latter is often combined with the constant-composition method, in which reagents are added to the system such as to compensate exactly for the consumption of solute by the growing crystals [37]. A particularly simple example of this method is the study of crystal growth of octacalcium phosphate, $Ca_4H(PO_4)_3,2.5H_2O$, by seeding a suspension of brushite, $CaHPO_4,2H_2O$, in very dilute phosphoric acid [38]. Brushite being the most reactive of the sparingly soluble calcium phosphates, it could be assumed that the solution was always saturated with respect to this compound. The progress of crystal growth was followed by pH-static titration with calcium hydroxide solution; the overall reaction is

$$6\ CaHPO_4,2H_2O(s) + 2\ Ca(OH)_2(aq) \rightarrow 2\ Ca_4H(PO_4)_3,2.5H_2O(s) + 11\ H_2O(l)$$

The system comprises 3 components (c), viz. $Ca(OH)_2$, H_3PO_4 and H_2O, and 2 phases (p) in equilibrium, i.e. solution and solid brushite, whence the number f of degrees of freedom according to Gibbs' phase rule

$$f = c + 2 - p \qquad (14)$$

is $f = 3$. Two variables with definite values are pressure and temperature. Hence, when pH is fixed the composition of the solution is constant, and the rate of consumption of calcium hydroxide represents the rate of crystal growth, at least as long as the number of growing crystals is constant and they grow homothetically, i.e. without change of shape. This latter may be the weak point, not only in seeded crystallization, but in all methods of mass crystallization. In experiments with seeding it is often observed that the apparent growth rate decreases with time, so a decision has to be made as to which rate be taken as representative. In the work described the initial rate was chosen.

3.2 Thermodynamic factors

A look at the equations (3), the definition of β, and (8), the Gibbs-Kelvin equation, points to $\ln \beta$ in growth rate expressions to be of thermodynamic origin. $\ln \beta$ may be replaced by $(m + x) \ln S$ (according to (5)) in (7), the equation for spiral growth, and in the preexponential factors in (10) and (12), the expressions for surface nucleation, incorporating the factor $m + x$ in the constants b, k_1 and k_2. The same substitution in (8) as well as in the exponents of (10) and (12) means that $\overline{s}$ should be redefined as the average area occupied by an ion in the growth layer.

The factor β in (10) accounts for assumed equilibrium between the supersaturated solution and the adsorbed growth units, and it leads to the factor $\beta^{1/3}$ in (12). It equals the ratio between actual and equilibrium surface concentration. Since in the electrolyte case β equals a *product* of ion activities divided by the solubility product according to (4), it must be replaced in this connection by S.

3.3 Kinetic factors

The last supersaturation-dependent factor in the kinetic expressions is β - 1. It is connected with the rate of advancement of steps. Unlike the thermodynamic factors considered above, we cannot give a general expression to replace β - 1, because we do not know in advance for a specific electrolyte which ion is rate-determining in step advancement. Christoffersen, Dohrup and Christoffersen studied crystal growth and dissolution of apatite [39] and found calcium ion to be rate-determining, though with some additional influence from the rate of dissociation of water molecules, providing the hydroxide ions of the apatite crystals. Ignoring the latter effect, β - 1 should be replaced by the difference between the concentrations of calcium in the actual and the saturated solution, in general terms c_M - $c_{M,eq}$.
The resulting equations are

$$R = b\left(c_M - c_{M,eq}\right)\ln \beta \qquad (15)$$

for spiral growth and

$$R = k_2 S^{1/3}\left(c_M - c_{M,eq}\right)^{2/3}\left(\ln \beta\right)^{1/6} \exp\left(-\frac{g\lambda^2 \overline{s}}{3(kT)^2 \ln \beta}\right) \qquad (16)$$

for polynuclear growth. The validity of the substitution made here will be discussed later.

3.4 Strategy of kinetic analysis

We assume that growth rates for different solution compositions have been measured. Tests for the different

growth laws are then carried out:

1. Plot R against S - 1. If the plot is linear, volume diffusion may be rate-determining. This may be checked by estimating diffusive mass transport. If this predicts a much higher growth rate than that found experimentally, the limiting cases leading to linear laws of the BCF theory and its extensions [8-12] should be considered. Thermal or kinetic roughening are alternatives.

2. Plot R against (c_M - $c_{M,eq}$) ln β, eq. (15). If the plot is linear, the growth mechanism is likely to be spiral growth. Either surface diffusion or integration into the growth site may be rate-determining. In the former case, known as the primary law, transition to linearity at higher supersaturation may be observed according to the BCF theory.

3. Divide R by the three supersaturation-dependent factors in front of the exponential in (16) and plot the logarithm of the result against 1/ln β. If the plot is linear, the growth mechanism is surface nucleation, and the edge free energy may be determined from the slope of the plot.

4. If in item 3 only a part of the plot corresponding to the high range of supersaturation is approximately linear, another mechanism operates together with surface nucleation, probably spiral growth if the slope is lower for the rest of the plot. Use is then made of the fact that the rate of growth by surface nucleation is negligibly low at low supersaturation, as is evident from Fig. 3. R_s is given by (15), and following the determination of the rate constant b from growth rates in the low range, it is calculated for the whole range of supersaturations. The results are inserted in (13), which is finally solved for R_n, given by (16).

5. If none of the above yields satisfactory linearity of the plots, other substitutions for β - 1 may be tried.

Valuable information on growth mechanisms is obtained if the system studied exhibits both spiral and surface nucleation growth kinetics, in particular if absolute growth rates have been determined. In mass crystallization this necessitates knowledge of crystal size distribution. Information on temperature dependence of rate constants (activation energy) is of great value as well.

4. Practical examples

The simplified Christoffersen theory and its generalization to spiral growth, expressed in eqs. (15) and (16), have turned out to account well for the crystal growth kinetics of cadmium phosphate [22,23], the copper phosphates Cu_2OHPO_4 (libethenite) and $CuHPO_4,H_2O$ [40] and brushite [41]. These substances were all studied by free crystallization, and pH was recorded during the process. Fig. 6 shows the data of Fig. 2 plotted according to item 2 above, including only the low range of supersaturations, and Fig. 7 shows the data of Fig. 3 plotted according to item 3. Both plots are linear within experimental uncertainty, indicating spiral growth and growth by surface nucleation, respectively.

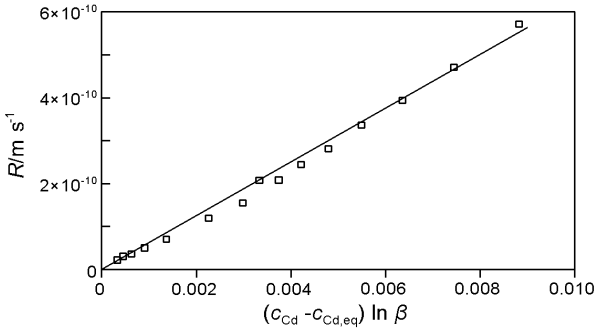

Fig. 6. Crystal growth rates of cadmium phosphate at low supersaturation plotted according to (15).

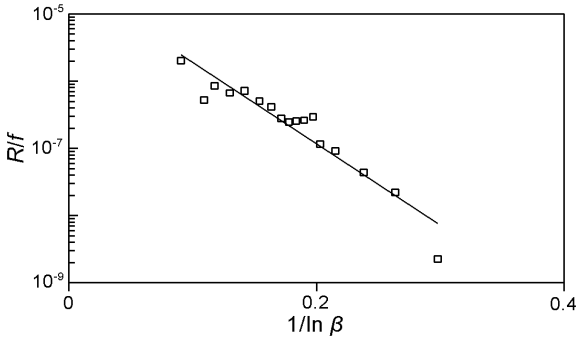

Fig. 7. Cadmium phosphate crystal growth rates plotted according to (16). The divisor f is the expression in front of the exponential.

As far as crystal growth is concerned, cadmium phosphate is a relatively uncomplicated substance to work with. For a substance with such low solubility it readily forms well-developed crystals, which means that crystal size distribution can be determined with simple methods of optical microscopy, and absolute growth rates are easily obtained. In the study of seeded growth of octacalcium phosphate in brushite suspension [38] the situation is somewhat different. The observed kinetics includes both spiral growth and surface nucleation, but for the latter it has not yet been possible to find an expression of the form (16) or (12) which could be fitted to the data in a satisfactory way. Instead the *ad hoc* solution of writing the preexponential factors as $[Ca^{2+}]c_P$ was chosen, the second factor being the total concentration of phosphate. Extensive analysis including temperature dependence of spiral growth led to the conclusion that the rate-determining step is the integration into the step of a growth unit with a time constant of the order of seconds. This corresponds quite well to the rate of dissociation of a proton from a hydrogen phosphate ion in solution [42].

5. Discussion

There are good reasons for assuming that metal ions are responsible for the rate-determining step in electrolyte crystal growth, at least with sparingly soluble electrolytes.

Nielsen analysed crystal growth kinetics of a large number of electrolytes and was able to express the growth rate in terms of the rate constant for integration of growth units into steps [20]. He could then demonstrate a good correlation of this quantity with the rate constant for dehydration of the metal ion, which ranges from 3×10^{-8} s^{-1} for Rh^{3+} and 5×10^{-7} s^{-1} for Cr^{3+} to 10^{10} s^{-1} for Ag^{+}, Tl^{+} and Pb^{2+}. On the average, integration was found to be 1000 times slower than dehydration. The extremely low value for Cr^{3+} manifests itself in the very low rate of the transformation

$$CrPO_4{,}6H_2O \rightarrow CrPO_4{,}4H_2O + 2\ H_2O$$

which takes several days [43,44].

The fact that the rate of crystal growth depends on metal ion concentration according to (16) does not exclude proton transfer as rate-determining, as the work of Christoffersen et al. shows [39]. Other evidence for the importance of this process was found in a study of the effect of magnetic field on the crystallization of sparingly soluble salts of both strong and weak acids [42]. An accelerating effect was found only for the latter, and only when the metal ion was diamagnetic. Further support was obtained by showing the absence of a magnetic effect on calcium carbonate crystallization at high pH, where CO_3^{2-} dominates over HCO_3^{-}, and in heavy water [45]. Cadmium phosphate showed the effect too, as expected [46], and still the dependence on metal ion concentration agreed with (16). A preliminary theory [47] suggests the explanation that approaching metal ions drive protons in the surface layer away from growth sites.

The case of seeded growth of octacalcium phosphate in brushite suspension [38] is still in need for a plausible mechanism as far as the preexponential factors in the expression for surface nucleation are concerned.

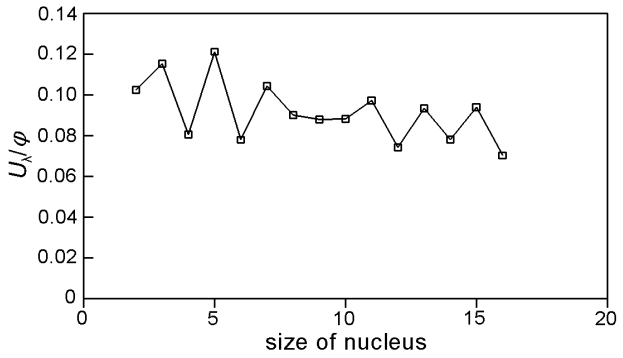

Fig. 8. Electrostatic edge energy U_λ of a surface nucleus on a crystal with NaCl structure. Size is given as number of ions, and φ is the energy of a pair of neighbouring ions.

Another problem is the size of the critical nucleus. Its size, expressed in number of growth units, may be derived from (8) and is given by

$$N^* = \frac{g\lambda^2\bar{s}}{(kT\ln\beta)^2} \tag{17}$$

For the results plotted in Figs. 3 and 7 we have λ = 26.4 pJ/m and N^* ranging from 1 to 7, taking g = 4 (square nucleus). Such a range of sizes of critical nuclei is not uncommon for crystal growth of sparingly soluble electrolytes by surface nucleation. However, considering the long range of electrostatic interactions, this small size raises the question of validity of the theory, at least so far as a definite value of λ is concerned.

The case may be elucidated by considering a small surface nucleus on a crystal-vacuum interface. The nucleus is thought as being built up by moving ions one by one from the growth site to the nucleus. The work equals the total edge energy, and division by the perimeter of the nucleus gives the edge energy per unit length. Fig. 8 shows the results for a crystal with NaCl structure, calculated for 2-16 ions, corresponding to 1-8 growth units. The variation of the contribution of purely electrostatic energy is seen to be relatively small. Including other interactions like Born repulsion and van der Waals forces is not likely to increase variations. On the other hand, λ is a free energy, so there is a negative contribution from entropy as well. Now the configurational entropy is largest for non-rectangular nuclei, which also have the highest electrostatic energy; thus, variations of free energy are likely to be significantly smaller than those of electrostatic energy. Finally, we consider crystal growth not from the vapour, but from solution. The negative adhesion energy is still another important contribution likely to suppress size-dependent variations in edge free energy of a nucleus. Hence there is no reason to believe that the theory is not consistent with experiments.

We may notice, however, that the plot in Fig. 7 exhibit a few deviations from strict linearity. Such irregularities are not uncommon in this kind of plots of electrolyte crystal growth kinetics. They may arise from certain sizes or configurations of small nuclei being particularly favourable or unfavourable energetically, yielding an edge free energy which is lower or higher, respectively, than the average value. An unusually strong manifestation of this effect was observed in heterogeneous nucleation of octacalcium phosphate on brushite, where the dependence of induction time, i.e. time lag in nucleation, was found to follow a distinct step function rather than a continuous function [48].

References

[1] W. Kossel, Nachr. Ges. Wiss. Göttingen, Math.-Phys. Kl., 135 (1927).
[2] I. N. Stranski, Z. phys. Chem. **136**, 259 (1928).
[3] N. F. Mott, R. W. Gurney, Electronic Processes in Ionic Crystals, ch. 1, Clarendon Press, Oxford (1940).
[4] R. Shuttleworth, Proc. Phys. Soc. London **62A**, 167 (1949).

[5] H. E. Lundager Madsen, J. Crystal Growth **112**, 458 (1991).
[6] H. E. Lundager Madsen, The Crystal-Water Interface of an Electrolyte, in: Meccanismi della crescita cristallina: fondamenti e applicazioni, 366-379, D. Aquilano, G. Artioli, M. Moret, Eds., Università degli Studi di Milano (2003).
[7] H. E. Lundager Madsen, J. Crystal Growth **85**, 377 (1987).
[8] W. K. Burton, N. Cabrera, F. C. Frank, Phil. Trans. Roy. Soc. London A **243**, 299 (1951).
[9] A. A. Chernov, Usp. Fiz. Nauk **73**, 277 (1961); Sov. Phys. Usp. **4**, 116 (1961).
[10] G. H. Gilmer, R. Ghez, N. Cabrera, J. Crystal Growth **8**, 79 (1971).
[11] P. Bennema, G. H. Gilmer, Kinetics of crystal growth, in: Crystal Growth, an Introduction, 263-327, P. Hartman, Ed., North-Holland, Amsterdam (1973).
[12] J. P. van der Eerden, J. Crystal Growth **56**, 174 (1982).
[13] N. Cabrera, M. M. Levine, Phil. Mag. **1**, 450 (1956).
[14] E. Budevski, G. Staikov, V. Bostanov, J. Crystal Growth **29**, 316 (1975).
[15] R. Becker, W. Döring, Ann. Physik **24**, 719 (1935).
[16] M. Volmer, Kinetik der Phasenbildung, Steinkopf, Leipzig (1939).
[17] R. Kaischev, Acta Phys. Hung. **8**, 75 (1957).
[18] W. B. Hillig, Acta Met. **14**, 1868 (1966).
[19] B. Simon, A. Grassi, R. Boistelle, J. Crystal Growth **26**, 77 (1974).
[20] A. E. Nielsen, J. Crystal Growth **67**, 289 (1984).
[21] G. H. Gilmer, J. Crystal Growth **36**, 15 (1976).
[22] H. E. Lundager Madsen, B. Tranberg Christensen, J. Crystal Growth **237-239**, 60 (2002).
[23] H. E. Lundager Madsen, J. Crystal Growth **244**, 349 (2002).
[24] J. D. O'Rourke, R. A. Johnson, Anal. Chem. **27**, 1699 (1955).
[25] A. E. Nielsen, J. Colloid Sci. **10**, 576 (1955).
[26] A. E. Nielsen, Kinetics of Precipitation, Pergamon, Oxford (1964).
[27] P. T. Cardew, J. Crystal Growth **57**, 391 (1982).
[28] S. Troost, J. Crystal Growth **13/14**, 449 (1972).
[29] K. Tsukamoto, J. Crystal Growth **61**, 199 (1983).
[30] K. Tsukamoto, I. Sunagawa, J. Crystal Growth **71**, 183 (1985).
[31] A. A. Chernov, I. L. Smol'sky, V. F. Parvov, Yu. G. Kuznetsov, V. N. Rozhansky, Kristallografiya **25**, 821 (1980); Sov. Phys. Crystallogr. **25**, 469 (1980).
[32] A. A. Chernov, L. N. Rashkovich, A. A. Mkrtchan, J. Crystal Growth **74**, 101 (1986).
[33] K. Onuma, K. Tsukamoto, I. Sunagawa, J. Crystal Growth **100**, 125 (1990).
[34] J. J. De Yoreo, T. A. Land, L. N. Rashkovich, T. A. Onischenko, J. D. Lee, O. V. Monovskii, N. P. Zaitseva, J. Crystal Growth **182**, 442 (1997).
[35] T. N. Thomas, T. A. Land, T. Martin, W. H. Casey, J. J. De Yoreo, J. Crystal Growth **260**, 566 (2004).
[36] H. Møller, H. E. Lundager Madsen, J. Crystal Growth **71**, 673 (1985).
[37] Z. Amjad, P. Koutsoukos, M. B. Thomson, G. H. Nancollas, J. Dental Res. **57**, 909 (1978).
[38] H. E. Lundager Madsen, Acta Chem. Scand. A **36**, 239 (1982).
[39] M. R. Christoffersen, J. Dohrup, J. Christoffersen, J. Crystal Growth **186**, 283 (1998).
[40] H. E. Lundager Madsen, J. Crystal Growth **275**, e191 (2005).
[41] H. E. Lundager Madsen, J. Crystal Growth **310**, 2602 (2008).
[42] H. E. Lundager Madsen, J. Crystal Growth **152**, 94 (1995).
[43] H. Schiff, Z. anorg. Chem. **43**, 304 (1905).
[44] A. F. Joseph, W. N. Rae, J. Chem. Soc. **111**, 196 (1917).
[45] H. E. Lundager Madsen, J. Crystal Growth **267**, 251 (2004).
[46] H. E. Lundager Madsen, J. Crystal Growth **263**, 564 (2004).
[47] H. E. Lundager Madsen, J. Crystal Growth **305**, 271 (2007).
[48] H. E. Lundager Madsen, Acta Chem. Scand. A **37**, 25 (1983).

*Corresponding author: helm@life.ku.dk